Vibronic structure of the cyclopentadienyl radical and its nonrigid van der Waals cluster with nitrogen

S. Sun and E. R. Bernstein

Vibronic structure of the cyclopentadienyl radical and its nonrigid van der Waals cluster with nitrogen

S. Sun and E. R. Bernstein

Department of Chemistry, Colorado State University, Fort Collins, Colorado 80523

Fluorescence excitation and two color mass resolved excitation spectroscopy are employed to study the $D_1(^2A_2'') \leftarrow D_0(^2E_1'')$ vibronic transitions of the cyclopentadienyl radical (cpd) and its van der Waals cluster with nitrogen. The radical is created by photolysis of the cyclopentadiene dimer and cooled by expansion from a supersonic nozzle. The $cpd(N_2)_1$ cluster is generated in this cooling process. Mass resolved excitation spectra of cpd are obtained for the first 1200 cm^{-1} of the $D_1 \leftarrow D_0$ transition. The excitation spectrum of $cpd(N_2)_1$ shows a complicated structure for the origin transition. With the application of hole burning spectroscopy, we are able to assign all the cluster transitions to a single isomer. The features are assigned to a 55 cm^{-1} out-of-plane van der Waals mode stretch and contortional (rotational) motions of the N_2 molecule with respect to the cpd radical. Empirical potential energy calculations are used to predict the properties of this cluster and yield the following results: (1) the N_2 molecular axis is perpendicular to the cpd fivefold axis and parallel to the plane of the cpd ring with the two molecular centers of mass lying on the fivefold ring axis; (2) the binding energy of $cpd(N_2)_1$ is 434 cm^{-1}; and (3) the rotational motion of the N_2 molecule is essentially unhindered about the cpd fivefold axis. The molecular symmetry group $D_{5h}(MS)$ is applied to the nonrigid cluster, and optical selection rules exclude even$\leftrightarrow$odd transitions ($\Delta n = 0, \pm 2, \pm 4,...$ allowed) between the different contortional levels. Tentative assignments are given to the observed contortional features based on these considerations. The barrier to internal rotation is also small in the excited state. The results for the $cpd(N_2)_1$ van der Waals cluster are compared to those for the benzene $(N_2)_1$ and benzyl radical $(N_2)_1$ clusters. © *1995 American Institute of Physics.*

I. INTRODUCTION

Supersonic jet laser spectroscopy has had a major impact on the study of three important and rich systems; reactive intermediates,[1] nonrigid molecules,[2] and van der Waals molecules.[3] In essence, isolation and cooling have allowed these species to be accessed under conditions that generate long lifetimes, sharp transitions, controlled dynamics, and ready detection. Studies of nonrigid molecules, reactive intermediates (radicals, carbenes, nitrenes), and van der Waals clusters of even complex and large species now become relatively straightforward. In fact we are just learning how to deal with these more complex systems as more subtle data are generated for them.[4]

Open-shell reactive intermediates play a fundamental role in many gas and condensed phase chemical reactions. The cpd radical, $C_5H_5\cdot$, is a simple, but reactive, cyclic polyene with a degenerate ground state, $^2E_1''$ in D_{5h} point group symmetry. Cpd also serves as a ligand in organometallic compounds. Engleman and Ramsey[5] and Nelson *et al.*[6] obtained UV spectra of cpd with reasonable resolution in a static cell, and a number of theoretical calculations at different levels of sophistication have also been reported for this radical.[7] Miller's group has conducted a series of high resolution spectroscopic studies of the 0_0^0 transition of cpd employing supersonic cooling and a ring dye laser. By photolyzing suitable molecular precursors and collecting laser induced fluorescence, they have obtained rotationally resolved electronic spectra of both protonated and deuterated cpd radicals,[8,9] as well as some substituted cpds.[10,11] Rota-

tional constants, Coriolis coupling constants, and the magnitude of the Jahn–Teller effect in the degenerate ground states of cpd have been determined.[10] In addition this group has reported and analyzed spectra of van der Waals complexes of cpd with different inert gas atoms (He,Ne).[12]

Our laboratory is also engaged in the study of reactive intermediates, and we have recently reported spectra of the benzyl and CN-cpd radicals.[13] In particular, the benzyl radical, and its van der Waals clusters, have been studied in considerable detail. The benzyl radical has two excited electronic states ($1\,^2A_2$ and $2\,^2B_2$) separated by $\sim$400 cm^{-1} near 22 000 cm^{-1} and an ionization energy of 7.24 eV.[13] Solvation of the benzyl radical with various nonpolar small molecules and hydrocarbons shows a systematic red shift for the origin of the van der Waals clusters.[14] The clusters' binding energies are roughly between 400 and 1000 cm^{-1}. Excited state reactivity for the benzyl radical with unsaturated hydrocarbons (e.g., ethylene) has been demonstrated both experimentally and theoretically.[15]

Another focus of our efforts has been on nonrigid molecules and van der Waals clusters. In these studies we have determined rotor potentials for different alkyl substituted benzenes and pyrazines and pyridines[16] and have investigated the lowest energy conformations of many other nonrigid systems.[17] Large amplitude motion in van der Waals clusters can be predicted on the basis of potential surface calculations but it is often difficult to detect spectroscopically.[18] Nevertheless, such motion becomes quite clear for systems with high symmetry and properly

aligned internal rotor axes (i.e., small hindering potentials). Such is the case for N_2, CO, and CO_2 clustered to benzene and N_2 clustered to the benzyl radical.[14,19] Contortional transitions can be observed for these systems in the vibronic spectrum of the clusters. Additionally, both microwave and rovibronic spectroscopy have shown affects of this internal cluster contortional freedom on the external rotational spectra of the benzene $(N_2)_1$ cluster.[20] For the benzene $(N_2)_1$ clusters, the nitrogen molecule lies above the plane of the benzene ring with its molecular bond axis perpendicular to the out-of-plane C_6 axis of the benzene molecule. The center of mass of the nitrogen molecule lies on the C_6 axis of benzene. In the ground electronic state of the cluster, the nitrogen rotational motion is unhindered and in the S_1 electronic state, the sixfold potential barrier is ~20 cm^{-1}. For the benzyl radical $(N_2)_1$ cluster the barrier to N_2 rotation is ~15 cm^{-1} in both D_1 and D_0 electronic states. The out-of-plane motion for the N_2 molecule is ~60 cm^{-1} for the benzene cluster and ~43 cm^{-1} for the benzyl radical argon cluster.

We report in this paper the continuation of these efforts with the radical cpd and its cluster with N_2. Both fluorescence excitation and mass resolved excitation spectra are presented for the unsolvated and solvated radical. The excitation spectra for cpd are discussed and partially assigned up to 1200 cm^{-1} above the 0_0^0 transition. The cpd$(N_2)_1$ cluster excitation spectrum about the origin transition region is interpreted with the aid of model calculations and molecular symmetry group $[D_{5h}(MS)]$ considerations. The fluorescence signal intensity for the cpd radical is quite intense. The 0_0^0 transition at 338.14 nm (29 573 cm^{-1}) is the most intense vibronic band probed in the wavelength region. The ionization threshold for the cpd radical is 8.41 eV,[21] but the cross section for ionization appears to be small near threshold. Mass resolved excitation spectra are therefore obtained for both the cluster and the bare radical at ~9.3 eV total ionization energy. At this experimental ionization energy, the cluster ion dissociates so the cpd$(N_2)_1$ spectra appear in the cpd mass channel. To compensate for the concomitant loss of mass resolution, fluorescence detected hole burning/population labeling data are collected for the cluster to distinguish and assign the complex features of the cpd$(N_2)_1$ cluster excitation spectrum. By saturating a specific vibronic feature in the cluster spectrum with a pump laser and monitoring the decrease of signal intensity arising from a probe laser, hole burning spectroscopy can be used to identify spectral features associated with different species. We are thus able to associate all features in the cpd$(N_2)_n$ cluster spectrum with a single cluster size ($n=1$) and geometry.

II. EXPERIMENTAL PROCEDURES

The experimental setup has been described fully previously for the spectroscopic study of the benzyl radical and its clusters.[14] Below we simply outline a few of the procedures to give an overview of the experimental approach taken.

The cpd radical is generated by 193 nm laser photolysis of dicyclopentadiene in a flow of He gas expanded through a pulsed supersonic nozzle. The excimer laser output is mildly focused at the nozzle throat. The excitation laser is a Nd:YAG pumped dye laser; a 1:1 mixture of DCM and LDS

698 (Exciton) is used to cover the wavelength region 682–650 nm. This fundamental output of the dye laser is doubled to reach 341–325 nm. The excitation beam is mildly focused 1 cm downstream of the nozzle for fluorescence studies and at the ionization region of the time-of-flight mass spectrometer for mass resolved studies. For mass resolved spectra, the ionization dye laser has an active medium of R590, the output of which is double and mixed with Nd:YAG fundamental (1064 nm) to generate ~220 nm radiation. The cpd$(N_2)_1$ signal appears in the bare radical mass channel (65 amu) due to cluster ion fragmentation.

Hole burning experiments are done with two lasers of similar wavelength output around the 0_0^0 transition of cpd. The two lasers have a hole burning to probe intensity ratio of roughly 5 to 1. The two laser beams propagate nearly collinear and are separated in time by roughly 600 ns. Since the D_1 bare radical excited state has a lifetime of about 60 ns, this time displacement ensures that fluorescence caused by the hole burning laser is not observed with the probe laser generated signal.

The detection system for the mass resolved spectra is the same as presented for the benzyl radical study. The fluorescence signal is detected by an RCA C31034A02 phototube, the output of which is amplified by a fast preamplifier. Both ion and fluorescence signals are sent to a digitizer or a boxcar integrator and then to a computer for recording. Two digital delay generators are used to control the timing of the experiment.

Dicylopentadiene is obtained from Aldrich Chemicals and used without purification. The sample is maintained at approximately room temperature during the experiment.

III. CALCULATIONAL PROCEDURES

A. Potential energy calculation: Cluster binding energy and geometry

Empirical potential energy calculations have been shown to render quite reasonable estimates of cluster geometry and binding energy for both closed-shell[19,22] and open-shell[14] systems. Even excited state estimates for Rydberg[23] and π^*[14] states seem to give results that are consistent with observations. Using the empirical atom–atom Lennard-Jones 6-12-1 potential format, the binding energy of van der Waals clusters can be expressed as follows:

$$V_{BE}=\frac{1}{2}\sum_{j=1}^{n}\sum_{i=1}^{m}(A^{ij}/r_{ij}^{12}-C^{ij}/r_{ij}^6+e_ie_j/r_{ij})=V_{6\text{-}12}+V_C,$$

(1)

in which r_{ij} is the distance between atoms i and j of different molecules, A^{ij} and C^{ij} are empirical parameters associated with different types of atoms (C,H,...) and e_i,e_j are the partial charges of atoms i and j, respectively.[22,24] Nitrogen atoms in N_2 should have no partial charge; however, to reproduce the N_2 quadrupole moment,[25] a charge distribution is introduced such that the atomic sites have charges of $+0.377e$ and two charges of $-0.377e$ are placed on the molecular axis 0.25 Å from each end of the molecule.[26] $V_{6\text{-}12}$ is the empirical term for the pure van der Waals interaction and V_C expresses the Coulomb component of the potential
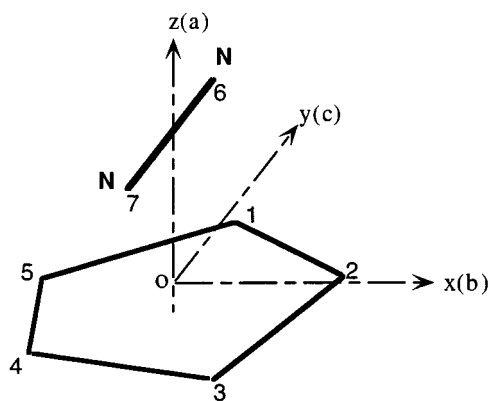
FIG. 1. Schematic diagram of the structure of $cpd(N_2)_1$ van der Waals cluster. The five hydrogen atoms are omitted for simplicity. The molecule fixed coordinate system is also shown in the diagram.
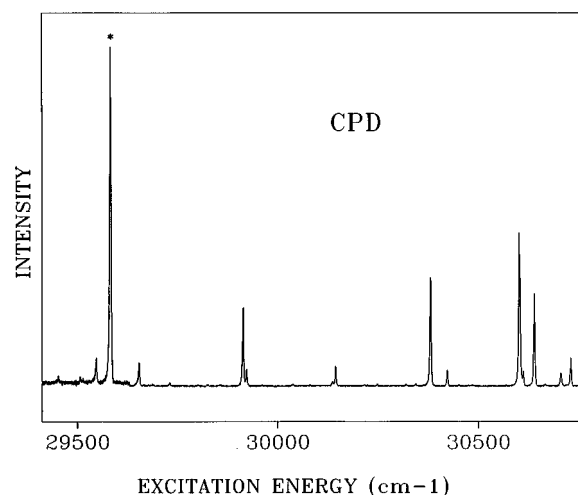

FIG. 2. Two-color MRES of the cpd radical. The feature marked with an asterisk is the radical origin band of $D_1 \leftarrow D_0$ transition.

energy associated with the interaction of the partial atomic charges on different molecules. In the calculation each molecule is assumed to be rigid; cpd has a D_{5h} geometry with internuclear distances given in Ref. 27. The results indicate that at the potential minimum the N_2 molecule lies horizontally on top of the cpd plane (N_2 bond axis parallel to cpd plane), with its center of mass 3.36 Å above the center of mass of the cpd ring (see Fig. 1) on the fivefold out-of-plane ring axis. By rotating the nitrogen molecule about the fivefold axis perpendicular to the cpd ring, one obtains the potential barrier to such internal rotational or contortional motion for the electronic ground state.

B. N_2 contortional motion

The internal rotation of N_2 on top of an aromatic hydrocarbon ring has been investigated in detail previously.[14,19] Assuming that the nitrogen molecule rotates around the vertical axis passing through both centers of mass of the molecules, the motion can be described by a simple one-dimensional rotor with the Schrödinger equation,

$$\left[-B \frac{\partial^2}{\partial \Theta^2} + V(\Theta) \right] \Psi_n(\Theta) = E_n \Psi_n(\Theta), \qquad (2)$$

in which Θ is the torsional angle for the N_2 rotor, B is the N_2 rotational constant ($h/8\pi^2 cI \sim 2$ cm^{-1}), and I is the reduced moment of inertia. Since N_2 lies on top of the cpd ring at the high symmetry position, the potential barrier for rotation has a tenfold symmetry and can be approximately represented as

$$V(\Theta) = \frac{1}{2} V_{10}[1 - \cos(10\Theta)], \qquad (3)$$

in which V_{10} is the tenfold potential barrier height for this motion. When $V = 0$ (a free rotor) the solution to Eq. (2) takes the form

$$\psi_k(\Theta) = \frac{1}{\sqrt{2\pi}} e^{\pm ik\Theta} \qquad (4)$$

and

$$E_k(\Theta) = k^2 B \quad (k = 0, \pm 1, \pm 2, \ldots). \qquad (5)$$

For the hindered N_2 rotor Hamiltonian [Eq. (2)], the eigenfunctions and eigenvalues are found within a basis set of 31 free rotor functions ($k = 0, \pm 1, \ldots, \pm 15$) such that

$$\Psi_n(\Theta) = \sum_{k=-15}^{15} C_{nk} \psi_k(\Theta) = \frac{1}{\sqrt{2\pi}} \sum_{k=-15}^{k=+15} C_{nk} e^{\pm ik\Theta}. \qquad (6)$$

The potential barrier V_{10} is treated as a parameter and adjusted to fit the experimental results.

Molecular symmetry group theory[28] is applied to this system to understand and develop the energy level structure in each electronic state and to obtain optical transition selection rules. Assuming that the only feasible contortional motion for the $cpd(N_2)_1$ cluster is the rotation of the nitrogen molecule about the C_5 cpd ring axis, the molecular symmetry group contains 20 feasible permutation-inversion operations. These operations comprise the $D_{5h}(MS)$ group which is isomorphic to the D_{5h} point group. Detailed symmetry considerations will be presented for this case in the following sections.

IV. RESULTS AND DISCUSSION

A. Excitation spectrum of cpd

The two-color mass resolved excitation spectrum of the supersonic expansion cooled cpd radical for the first 1200 cm^{-1} of the $D_1(^2A_2'') \leftarrow D_0(^2E_1'')$ (point group symmetry notation) transition is presented in Fig. 2. A number of vibronic transitions are observed in this region and the transition energies, intensities, and some tentative assignments are presented in Table I. The strongest transition is the 0_0^0 band which appears at 29 573 cm^{-1}. The cpd radical has a lifetime (measured by the 0_0^0 transition) of 65 ns. This is in agreement with the result of Ref. 29. The fluorescence excitation spectrum in this region is identical (with the exception of some intensity variation) to that shown in Fig. 2.

TABLE I. Vibronic bands for the cpd radical $D_1 \leftarrow D_0$ transition.

Peak position (cm^{-1})	Spectral shift (cm^{-1})	Relative intensity	Assignment[a]
29 537	−36	7	
29 573	0	100	0^0_0
29 644	71	7	
29 904	331	16	ν_{14}
29 912	339	5	
30 135	562	6	
30 372	799	32	ν_2
30 413	840	5	
30 593	1020	46	$3\nu_{14}, \nu_{11}$
30 603	1034	4	$\nu_{14} + \nu_2$
30 631	1058	28	ν_{10}
30 698	1125	4	ν_5
30 722	1149	8	

[a]References 6, 29, 30.

TABLE II. Transition energies and relative spectral shifts of cpd(N$_2$)$_1$ vdW cluster in the origin band region.

Peak number	Transition energy[a]	Relative spectral shift
1a	−167.3	0
1b	−164.1	3.2
1c	−158.7	8.6
2a	−110.8	0
2b	−107.6	3.2
2c	−102.1	8.7
3a	−57.0	0
3b	−54.1	2.9
3c	−47.5	9.5

[a]Relative to the origin band of the cpd radical at 29 573 cm^{-1}.

B. Excitation spectrum of cpd(N$_2$)$_1$

Figure 3 shows the fluorescence excitation spectrum of the cpd(N$_2$)$_1$ van der Waals cluster in the origin region. Intensity of the cluster features is less than 10% of that of the cpd bare radical signal. The structure of each main feature in this spectrum is complex as can be seen in the enlargement section of Fig. 3. The cluster spectrum consists of three main groups of features separated by roughly 55 cm^{-1}. On closer inspection each of these three groups is composed of three additional peaks; one relatively intense band (a) at the low energy side of this structure; a closely spaced (~3 cm^{-1}) band (b) of medium intensity; and a higher energy feature (c) ~9 cm^{-1} from the first component of the triplet. These are referred to as 1a, b, c, 2a, b, c, and 3a, b, c in Fig. 3 and Table II.

By comparison with C$_6$H$_6$(N$_2$)$_1$ and C$_6$H$_5$CH$_2$(N$_2$)$_1$ cluster spectra, one can suggest that the three main features (1,2,3) are associated with the cpd/N$_2$ out-of-plane totally symmetric mode and that the three closely spaced features (a,b,c) are associated with internal rotation of the N$_2$ about the out-of-plane C_5 cpd ring axis. The closely spaced multiple peak structure is due to the electronic-contortional transitions from levels of D_0 to those of D_1.

Two-color MRES of cpd(N$_2$)$_1$ did not yield any signal in the cluster mass channel (65+28=93 amu) due to fragmentation of the cluster ion with ~7000 cm^{-1} of energy above the ionization threshold. The cluster spectra are, however, observed in the bare cpd mass channel. They are identical to those observed by fluorescence excitation. These data are insufficient to prove that all features observed are associated with the one to one cpd/N$_2$ cluster even though we can be certain that at least some of them are due to cpd(N$_2$)$_1$.

C. Hole burning spectrum of cpd(N$_2$)$_1$

One way to compensate for loss of mass resolution due to fragmentation of the cluster ion is to do a hole burning experiment. Since at least one of these main features (1,2,3) in the cluster spectrum is surely due to cpd(N$_2$)$_1$, this technique will show if the other features arise from the same ground state species. We can expect that perhaps some of the contortional fine structure (a,b,c) would not arise from the same ground state level due to selection rules and/or hot bands.[30] With this technique one cannot only distinguish between clusters of different masses and states, but also between clusters of different conformation. Our implementation of the usual hole-burning experiment is possible because the clusters are isolated in the molecular beam, and vibrational relaxation on the ground electronic state surface of C$_5$H$_5$(N$_2$)$_1$ is quite slow. The separation in time between the pump pulse and the probe pulse is long compared to fluorescence times, but short compared to ground state vibrational relaxation times at low total cluster vibrational excitation energy. Thus, the hole-burning process transfers population from the electronic and vibrational ground state to excited vibrations of the ground electronic state for the duration of the experiment.

The top panel (a) of Fig. 4 displays the hole burning spectrum of the cpd(N$_2$)$_1$ cluster. As a comparison, the fluorescence excitation spectrum of the cluster is presented in the
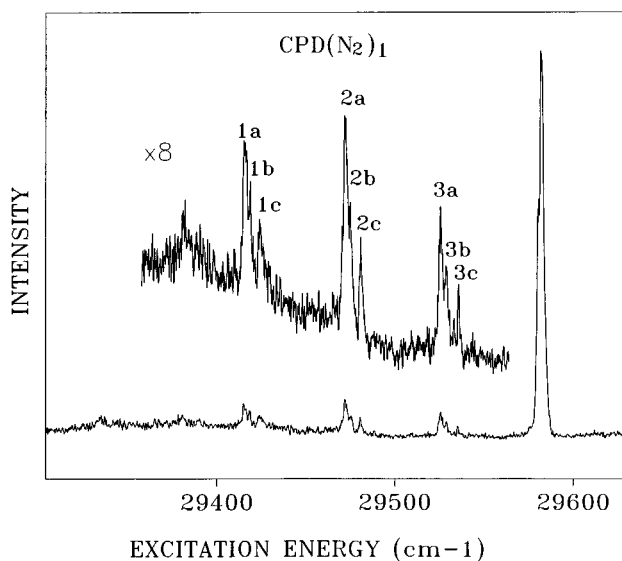
FIG. 3. FE spectrum of cpd(N$_2$)$_1$ van der Waals cluster. The strongest peak is the 0^0_0 band of the cpd radical. The cluster features are −170 to −50 cm^{-1} red shifted from the radical origin band. The insert shows the eightfold expanded cluster transition features.
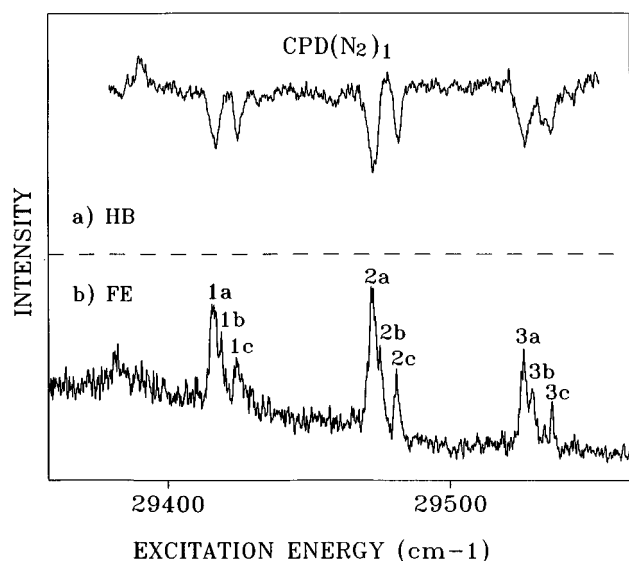
FIG. 4. (a) Hole burning, (b) FE spectrum of cpd$(N_2)_1$ van der Waals cluster in the radical origin band region. In the hole burning spectrum (a), the fluorescence signal depletion ratio is about 30%. The probe laser wavelength is fixed at the cluster transition band 2a, which is -111 cm^{-1} red shifted from the 0_0^0 band of the cpd radical.

FIG. 5. Diagram of the energy level structure of the N_2 internal rotation on top of the cpd ring ($B \approx 2.0$ cm^{-1}). The horizontal variable is the potential barrier parameter V_{10}. Note the loss of double degeneracy of the every fifth level.

bottom panel (b) of this figure. By monitoring the fluorescence induced by the probe laser, a series of spectral holes are burnt as the pump/hole burning laser excites the cluster species at the same ground state vibrational level as excited by the probe laser. These spectral holes [Fig. 4(a)] correspond exactly to the features 1,2,3a,c in the excitation spectrum. Clearly the features, 1,2,3a,c all derive from the same energy level of the one-to-one cluster which has only one conformation. The 1,2,3b features probably arise from another independent level of this single cluster species. The lowest energy broad features at $\sim$29 390 cm^{-1} may well be due to a higher order cluster. In the hole burning experiment, the probe laser is fixed at feature 2a (-111 cm^{-1} from the cpd 0_0^0), the most intense feature in the cpd$(N_2)_1$ spectrum, and the pump laser is tuned through the transitions (1a to 3c). The signal depletion can be as high as 30%. Since at these laser power levels little or no saturation exists for these transitions, about 1/3 of the ground state population has been depleted by the pump laser.

If all the main features (1,2,3) in the cpd$(N_2)_1$ spectrum are from the same cluster, they can be assigned as a Franck–Condon progression in a totally symmetric out-of-plane S_z stretch of the $N_2 \cdots$cpd van der Waals bond. As a comparison with $C_6H_6(N_2)_1$, $(CO)_1$, and $(CO_2)_1$ clusters, the S_z stretch is given as 60, 68, and 70 cm^{-1}, respectively.[19] The 55 cm^{-1} assignment for this mode in cpd$(N_2)_1$ is certainly consistent with the benzene cluster assignments.

Careful inspection of the hole burning spectrum suggests that the center bands (b) in each group of the S_z mode progression is missing. Although this is not completely unambiguous in Fig. 4 due to noise, several repeats of this spectrum do not reveal any hole burning at the b positions. Since each group of peaks is believed to correspond to the excitation of internal N_2 contortional motion, we suggest that
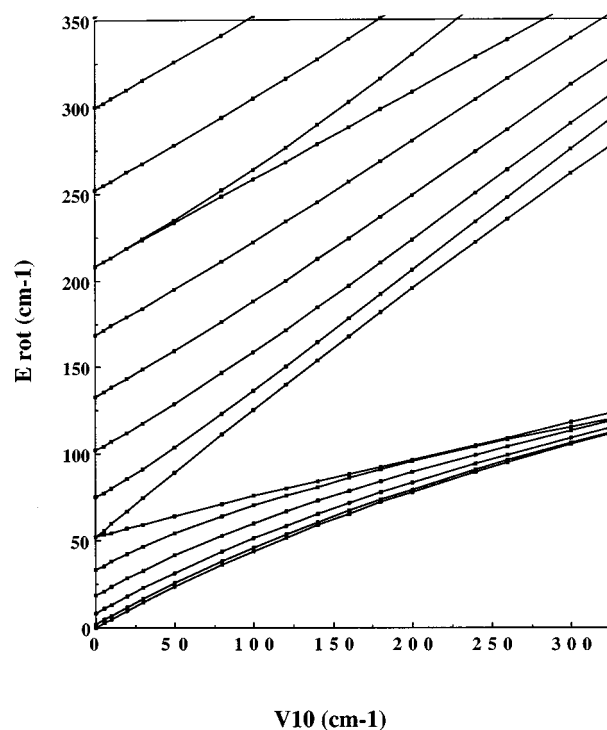
bands a and c originate from the same contortional level of the ground state while bands b arise from another ground state contortional level. Transitions 1,2,3b are too weak and too poorly resolved to observe the hole burning spectrum with any of them as a probe transition.

A hole burning experiment has also been performed for the bare cpd radical at its original band. When the probe laser is fixed at the cpd 0_0^0 transition and the hole burning pump laser is scanned, only a single sharp feature at the 0_0^0 position is observed. This implies that the bare cpd features at -36 cm^{-1} and $+71$ cm^{-1} in the spectrum belong to hot band transitions originating from populated cpd vibrational levels of the ground electronic state. The depletion change of the radical 0_0^0 transition is again roughly 30%.

D. Calculation results and symmetry considerations

The empirical potential energy calculations show that the energy minimum equilibrium structure for the cpd$(N_2)_1$ cluster has the N_2 molecule 3.36 Å above the cpd plane with the N–N bond axis parallel to the plane; the two molecular centers of mass lie on the fivefold ring axis in this geometry. The van der Waals and Coulomb interaction energies are -429 and -5 cm^{-1}, respectively, so that the total binding energy for the cluster with cpd in its ground state is 434 cm^{-1}. Rotation of the N_2 moiety about the out-of-plane z-axis (C_5 symmetry axis) of cpd generates potential energy variations of $\sim$0.01 cm^{-1}, so that N_2 is a one-dimensional free rotor in

TABLE III. Symmetry representations of the free rotor wave functions in group D_{5h}(MS).

Free rotor wave function $\psi_k{}^a$	Symmetry representation (Γ)
$k=0$	A_1'
$k=10m^b$	$A_1' + A_2'$
$k=10m\pm1$	E_1''
$k=10m\pm2$	E_2'
$k=10m\pm3$	E_2''
$k=10m\pm4$	E_1'
$k=10m\pm5$	$A_1'' + A_2''$

$^a\psi_k(\Theta) = (1/\sqrt{2\pi})e^{\pm ik\Theta}$.
$^b m$ is an integer.

the cpd$(N_2)_1$ cluster ground electronic state. Similar results are reported for $C_6H_6(N_2)_1$, $(CO)_1$, and $(CO_2)_1$, and $C_6H_5CH_2(N_2)_1$ clusters.[19]

The Schrödinger equation (2) for a hindered rotor has been solved for $C_5H_5(N_2)_1$ in a basis set of 31 free rotor states ($k=0,\pm1,\pm2,...,\pm15$) [Eq. (6)] with the tenfold barrier V_{10} [Eq. (3)] as a parameter. Figure 5 shows such an energy level structure for the internal N_2 molecule rotation as a function of the barrier height V_{10}. At $V_{10}=0$ all the rotational levels are doubly degenerate except the lowest one ($k=0$). With increasing V_{10}, the levels with index value $n=5,10,15,...$ split. This latter loss of degeneracy is due to the symmetry of these levels (A_1+A_2) in D_{5h}(MS). Such behavior is common in hindered rotor problems and has been demonstrated in the past.[19]

Table III gives the transformation properties of the free rotor basis eigenvectors in the D_{5h}(MS) molecular symmetry group. Note that the levels $k=10m$ and $10m\pm5$ have symmetry A_1+A_2 and thus split for $V_{10}\neq0$. Therefore the actual hindered rotor wave functions have the irreducible representations as follows: $0a_1',1e_1'',2e_2',3e_2'',4e_1',5_aa_1'',5_ba_2'',6e_1',7e_2'',8e_2',9e_1'',10_aa_2',10_ba_1',11e_1',12e_2',13e_2'',...$. If the molecule fixed axes are as given in Fig. 1, the symmetry representatives for the dipole moment components are $\Gamma_{Mz} = a_1'$ and $\Gamma_{(Mx,My)} = e_1'$. The antisymmetric representations, according to which the entire cluster eigenfunctions must transform, are $\Gamma_a = a_1'$ or a_2', for $+$ or $-$ parity, respectively. The D_{5h}(MS) character table is presented in Table IV.

In the D_{5h}(MS) group, the ground state D_0 and the first excited state D_1 of the cpd$(N_2)_1$ cluster transform according to the irreducible representations e_1' and a_1', respectively. Note that this is equivalent to the bare cpd electronic states (for the D_{5h} point group) D_0 and D_1 transforming according to E_1'' and A_2'', respectively. The 0_0^0 transition in the cluster (and the bare cpd) is thus allowed by the (xy) component of the dipole transition operator in each instance and is quite intense. To analyze the complicated excitation features (a,b,c in Figs. 3 and 4), which derive from transitions associated with the N_2 rotational excitation or contortional levels, the symmetry of such contortional levels must be considered. The optical selection rules derived for the overall transition depend on the matrix element

$$\langle \psi_{rot}^e \psi_{vib}^e \psi_{con}^e \psi_{el}^e | \mathbf{M} | \psi_{rot}^g \psi_{vib}^g \psi_{con}^g \psi_{el}^g \rangle \neq 0. \qquad (7)$$

Since $\Gamma_{el}^g = e_1'$ and $\Gamma_{el}^e = a_1'$ for the $D_1 \leftarrow D_0$ transition, we have, ignoring the external overall rotational levels of the cluster, which remain unresolved in these studies,

$$a_1' \otimes \Gamma_{con}^e \otimes \begin{bmatrix} a_1' \\ e_1' \end{bmatrix} \otimes \Gamma_{con}^g \otimes e_1' \supset a_1'. \qquad (8)$$

Electronic-contortional transition selection rules for the cpd$(N_2)_1$ cluster about the 0_0^0 transition derive from Eq. (8). For example, the $0a_1'$ level has allowed transition to $0a_1',2e_2',4e_1',6e_1',8e_2',10_aa_2',10_ba_1',...$ in the excited state D_1 while the level $1e_1''$ has allowed transitions to levels $1e_1'',3e_2'',5_aa_1'',5_ba_2'',7e_2'',9e_1'',11e_1'',...$ in the excited state D_1. In general, even $\leftrightarrow$ odd level transitions are forbidden because the selection rule excludes $' \leftrightarrow ''$ transitions.

The nuclear spin wave functions for the five hydrogen atoms ($I_H=1/2$) in cpd have the symmetry $8a_1' \oplus 6e_1' \oplus 6e_2'$, while the nitrogen molecule ($I_N=1$) nuclear spin wave functions have the symmetry $6a_1' \oplus 3a_1''$. The nuclear spin wave function for the five carbon atoms is of a_1' symmetry since $I_C=0$ for ^{12}C. Therefore the total nuclear spin statistical weights are

Γ_{nspin}	a_1'	a_2'	e_1'	e_2'	a_1''	a_2''	e_1''	e_2''
statistical weight	8	0	6	6	5	0	3	3

TABLE IV. The character table of the group D_{5h}(MS).

D_{5h}(MS)	E	(12345)	(13524)	(13)(45)*	(67)	(12345)(67)	(13524)(67)	(13)(45)(67)*	
	1	2	2	5	1	2	2	5	
Equiv. rot.	R^0	$R_z^{2\pi/5}$	$R_z^{4\pi/5}$	$R_{10\pi}^{\pi}$	R^0	$R_z^{2\pi/5}$	$R_z^{4\pi/5}$	$R_{10\pi}^{\pi}$	
A_1'	1	1	1	1	1	1	1	1	T_z
A_2'	1	1	1	-1	1	1	1	-1	
E_1'	2	2 cos 72°	2 cos 144°	0	2	2 cos 72°	2 cos 144°	0	(T_x,T_y)
E_2'	2	2 cos 144°	2 cos 72°	0	2	2 cos 144°	2 cos 72°	0	
A_1''	1	1	1	1	-1	-1	-1	-1	
A_2''	1	1	1	-1	-1	-1	-1	1	
E_1''	2	2 cos 72°	2 cos 144°	0	-2	-2 cos 72°	-2 cos 144°	0	
E_2''	2	2 cos 144°	2 cos 72°	0	-2	-2 cos 144°	-2 cos 72°	0	

Since $cpd(N_2)_1$ is a near-prolate asymmetric rotor, the rotational wave functions of this cluster transform as follows:

$K_a K_c$	ee	eo	oe	oo
Γ_{rot}	a_1'	a_2'	a_2''	a_1''

The complete internal wave function Φ_{int} of the cluster should transform as either a_1' or a_2' and thus

$$\Gamma_{rot} \otimes \Gamma_{vib} \otimes \Gamma_{cont} \otimes \Gamma_{elec} \otimes \Gamma_{nspin} \supset (a_1', a_2'). \quad (9)$$

This leads to the conclusion that, in the ground electronic state, all contortional levels can be populated.

The experimental results (Figs. 3 and 4) show three groups of transition features which are quite similar to each other. These groups (1,2,3) are assigned as a Franck–Condon progression in the symmetric stretch van der Waals mode in which the N_2 molecule moves along the out-of-plane z-axis, maintaining the symmetry of the cluster. Each group of transitions shows three main features (a,b,c in the figures); the center band b of these groups is missing from the 2a-detected hole burning spectrum of Fig. 4. This supports the conclusion that bands a and c originate from a common contortional level in the ground electronic state, probably, the $0a_1'$ level, while band b originates from a different contortional level, possibly the $1e_1''$ level, in the ground electronic state. Bands a and c of each symmetric stretch feature (0,1,2) are thereby assigned as contortional transition $0a_1' \leftarrow 0a_1'$ and $2e_2' \leftarrow 0a_1'$, respectively. The calculated separation between these two transitions is 8.3 cm^{-1} at $V_{10}=0$ in both electronic states, which is consistent with the experimental result, $\Delta_{ac} \sim 9$ cm^{-1}. As V_{10} increases in this model, the energy levels become less separated in the 0_0^0 region and the separation between these contortional transitions decreases. The similarity between the $V_{10}=0$ calculated a and c separation and that observed suggests that the barrier to N_2 contortion in the excited state is also quite small ($V_{10}^e \sim V_{10}^e \sim 0$ cm^{-1}). The most plausible assignment for the b bands is $1e_1'' D_1 \leftarrow 1e_1'' D_0$ but the $\Delta_{ab} \sim 3$ cm^{-1} is not clearly assignable as the expected value for this transition is ~ 0 cm^{-1}. Since the number of observed transitions is small, one cannot give a definitive assignment to all the contortional transition features. One can be certain, nonetheless, that the a,b,c features in Figs. 3 and 4 do indeed arise from N_2 contortional motion in both ground and excited electronic states and that the barriers to this contortion are quite small in both electronic states.

A comparison between these results for $cpd(N_2)_1$ and those reported for $C_6H_6(N_2)_1$ (Ref. 19) and $C_6H_5CH_2(N_2)_1$ (Ref. 14) proves to be both useful and interesting. The three clusters all have N_2 in roughly the same geometry with the N_2 bond axis lying parallel to the plane of the aromatic ring with an intermolecular center of mass to center of mass distance of 3.3–3.5 Å. The ground state binding energies are calculated to be 501, 520, and 434 cm^{-1} for the benzene, benzyl, and cpd/N_2 clusters, respectively. Experimental results for $C_6H_5CH_2(N_2)_1$ suggest that the calculated binding energy for this cluster is roughly 10% too high but the vibronic structure for this system is somewhat complex. The out-of-plane van der Waals symmetric stretch for these N_2 clusters is 60, 43, and 55 cm^{-1} for benzene, benzyl, and cpd, respectively. In the $cpd(N_2)_1$ cluster the three member Franck–Condon progression observed in this mode suggests that the geometry changes somewhat in the transition. A fourth member of this progression may be obscured by the 0_0^0 transition of the bare cpd.

These ostensibly similar clusters, benzene, benzyl, cpd with N_2, also evidence some important differences. First, the 0_0^0 of $C_6H_6(N_2)_1$ is blue shifted from that of benzene by 36 cm^{-1}; the cluster 6_0^1 transition is red shifted by 6 cm^{-1}. This difference in itself is quite unusual and is not fully understood. One possible suggestion for the 0_0^0 blue shifted origin of the $C_6H_6(N_2)_1$ cluster is that the observed feature at 0_0^0 (C_6H_6)+36 cm^{-1} is actually a vibronic feature associated with a nontotally symmetric van der Waals mode. This mode could aid in inducing the transition intensity as the 0_0^0 transition of C_6H_6 is forbidden. The radical cluster shifts are to the red at 17 and 167 cm^{-1} for benzyl and cpd, respectively. These two shifts are so different that one is not readily able to explain them in terms of the electronic structure differences in the cluster. Future, very accurate, high level *ab initio* calculations on these clusters might be able to shed some light on these cluster shifts. Second, the contortional barriers in the ground state of benzene and cpd nitrogen clusters are essentially zero while that for the benzyl radical-nitrogen clusters is ~ 12 cm^{-1}. The excited state barriers for benzene and cpd clusters are ~ 20 cm^{-1} and ~ 0 cm^{-1} and that for benzyl-nitrogen is ~ 23 cm^{-1}. These ground and excited state barriers would seem to have more to do with electronic structure than the ring substitution of the CH_2 group.

V. CONCLUSIONS AND SUMMARY

Mass resolved and fluorescence techniques are employed to study the vibronic structure of the cpd radical and its one-to-one van der Waals cluster with nitrogen. Empirical potential energy calculations are used to enhance understanding of the cluster excitation features. Since the $cpd(N_2)_1$ cluster fragments under the present experimental ionization conditions, hole burning experiments compensate for the associated loss of mass information. These latter studies demonstrate that all features observed for the cpd/N_2 cluster belong to a single cluster with the same mass and geometry.

The mass resolved excitation spectrum for the cpd radical is presented up to 1200 cm^{-1} above the 0_0^0 transition at 29 573 cm^{-1}. A number of vibronic features of this spectrum are assigned. The excitation spectrum of $cpd(N_2)_1$ exhibits complicated features around the cluster origin band. With the aid of hole burning spectroscopy, three groups of transitions can be assigned to a Franck–Condon progression in the cpd-N_2 van der Waals stretch mode of a single geometry $cpd(N_2)_1$ cluster. The closely spaced structure comprising these main bands is assigned to contortional transitions of the N_2 about the cpd out-of-plane z-axis.

Calculations give the cluster geometry as presented in Fig. 1 (nitrogen band axis parallel to and above the plane of the cpd with the N_2 center of mass on the C_5 axis of the ring) and a cluster binding energy of 434 cm^{-1}. The contortional

barrier in the ground state is ~0 cm^{-1}. Experiments suggest that the excited state barrier is also nearly zero. The D_{5h}(MS) group is applied to analyze the contortional motion and derive spectroscopic selection rules; even↔odd transitions ($\Delta n = \pm 1, \pm 3,...$) are forbidden for the contortions.

The cpd$(N_2)_1$, $C_6H_6(N_2)_1$, and $C_6H_5CH_2(N_2)_1$ results are compared and contrasted, with regard to binding energy, cluster shift, and potential barrier for both electronic states. The bond energies for these clusters are similar, but the cluster shifts are quite different. The barriers are all small and relate more to electronic structure that ring substituents. Future studies of cpd clusters in our laboratory will relate nonrigid behavior, cluster dynamics, and cluster chemistry.

ACKNOWLEDGMENT

[1] See, for example (a) S. C. Foster and T. A. Miller, J. Phys. Chem. **93**, 5986 (1989); (b) P. C. Engleking, Chem. Rev. **91**, 399 (1991); (c) E. R. Bernstein, J. Phys. Chem. **96**, 10 105 (1992).

[2] See, for example (a) M. Ito, J. Phys. Chem. **91**, 517 (1987); (b) P. J. Breen, J. A. Warren, E. R. Bernstein, and J. I. Seeman, J. Chem. Phys. **97**, 1917 (1987); (c) **87**, 1927 (1987).

[3] *Atomic and Molecular Clusters*, edited by E. R. Bernstein (Plenum, New York, 1990).

[4] For a recent review, see the special November issue of Chem. Rev. **94**, 1721 (1994): van der Waals Molecules II.

[5] R. Engleman, Jr. and D. A. Ramsey, Can. J. Phys. **48**, 964 (1970).

[6] H. H. Nelson, L. Pasternack, and J. R. McDonald, Chem. Phys. **74**, 227 (1983).

[7] See, for example, W. T. Borden and E. R. Davidson, J. Am. Chem. Soc. **101**, 3773 (1979).

[8] L. Yu, S. C. Foster, J. M. Williamson, M. C. Heaven, and T. A. Miller, J. Phys. Chem. **92**, 4263 (1988).

[9] L. Yu, J. M. Williamson, and T. A. Miller, Chem. Phys. Lett. **162**, 431 (1989).

[10] L. Yu, D. W. Cullin, J. M. Williamson, and T. A. Miller, J. Chem. Phys. **95**, 804 (1991).

[11] D. W. Cullin, L. Yu, J. M. Williamson, and T. A. Miller, J. Phys. Chem. **96**, 89 (1992).

[12] L. Yu, J. M. Williamson, S. C. Foster, and T. A. Miller, J. Chem. Phys. **97**, 5273 (1992).

[13] H. S. Im and E. R. Bernstein, J. Chem. Phys. **95**, 6326 (1991).

[14] R. Disselkamp and E. R. Bernstein, J. Chem. Phys. **98**, 4339 (1993).

[15] R. Disselkamp and E. R. Bernstein, J. Phys. Chem. **98**, 7260 (1994).

[16] J. I. Seeman, J. B. Paine, III, H. V. Sector, H. S. Im, and E. R. Bernstein, J. Am. Chem. Soc. **114**, 5269 (1992).

[17] (a) K. S. Law and E. R. Bernstein, J. Chem. Phys. **82**, 2856 (1985); (b) P. J. Breen, E. R. Bernstein, and J. I. Seeman, *ibid*. **87**, 3269 (1987); (c) P. J. Breen, J. A. Warren, E. R. Bernstein, and J. I. Seeman, J. Am. Chem. Soc. **109**, 3453 (1987); (d) H. S. Im and E. R. Bernstein, J. Chem. Phys. **88**, 7337 (1988).

[18] D. J. Nesbitt and R. Naaman, J. Chem. Phys. **91**, 3081 (1989).

[19] R. Nowak, J. A. Menapace, and E. R. Bernstein, J. Chem. Phys. **89**, 1309 (1988).

[20] (a) Th. Weber, A. M. Smith, E. Riedle, H. J. Neusser, and E. W. Schlag, Chem. Phys. Lett. **175**, 79 (1990); (b) P. Hobza, O. Bludsky, H. L. Selzle, and E. W. Schlag, J. Chem. Phys. **87**, 6223 (1993); (c) Y. Ohshima, H. Kohguchi, and Y. Endo, Chem. Phys. Lett. **184**, 21 (1991).

[21] F. P. Lossing and J. C. Traeger, J. Am. Chem. Soc. **97**, 1579 (1975).

[22] (a) J. A. Menapace and E. R. Bernstein, J. Phys. Chem. **91**, 2533 (1987); (b) S. Li and E. R. Bernstein, J. Chem. Phys. **95**, 1577 (1991).

[23] (a) Q. Y. Shang, P. O. Moreno, C. F. Dion, and E. R. Bernstein, J. Chem. Phys. **98**, 6769 (1993); (b) Q. Y. Shang, C. F. Dion, and E. R. Bernstein, *ibid*. **101**, 118 (1994); (c) Q. Y. Shang and E. R. Bernstein, Chem. Rev. **84**, 2015 (1994).

[24] F. A. Momany, L. M. Carruthers, R. F. McGuire, and H. A. Scheraga, J. Phys. Chem. **78**, 1595 (1974); G. Nemethy, M. S. Pottle, and H. A. Scheraga, *ibid*. **87**, 1883 (1983), and references therein.

[25] F. P. Billingsley and M. Krauss, J. Chem. Phys. **60**, 2767 (1974).

[26] D. E. Williams and S. R. Cox, Acta Crystallogr. B **40**, 404 (1984).

[27] L. Yu, D. W. Cullin, J. M. Williamson, and T. A. Miller, J. Chem. Phys. **98**, 2682 (1993).

[28] P. R. Bunker, *Molecular Symmetry and Spectroscopy* (Academic, New York, 1979).

[29] L. F. DiMauro, M. Heaven, and T. A. Miller, Chem. Phys. Lett. **124**, 489 (1986).

[30] D. Purins and H. F. Feeley, J. Mol. Struct. **22**, 11 (1974).